Journal of Translational Medicine

RESEARCH Open Access

STYK1 mediates NK cell anti-tumor response through regulating CCR2 and trafficking

Junming He[1,2], Yuexi He[7], Ruojia Biao[8,9,10,11], Yuqing Wei[8,9,10,11], Zhongjun Dong[3,4,5,6,7,13*] and Juan Du[8,9,10,11,12*]

Abstract

The serine/threonine/tyrosine kinase 1 (STYK1) is a receptor protein-tyrosine kinase (RPTK)-like molecule that is detected in several human organs. STYK1 plays an important role in promoting tumorigenesis and metastasis in various cancers. By analyzing the expression of RTKs in immune cells in the database of 2013 Immunological Genome Project, we found that STYK1 was principally expressed in NK cells. In order to investigate the function of STYK1, we used CRISPR/Cas9 technology to generate STYK1-deleted mice, we found STYK1 deletion mice have normal number, development, and function of NK cells in spleen and bone marrow in tumor-free resting state. To examine the tumor surveillance of STYK1 in vivo, we utilized a variety of tumor models, including NK cell-specific target cell (ß2M and RMA-S) clearance experiments in vivo, subcutaneous and intravenous injection of B16F10 melanoma model, and the spontaneous breast cancer model MMTV-PyMT. Surprisingly, we discovered that deletion of the oncogenic STYK1 promoted the four-model tumor progression, and we observed a reduction of NK cell accumulation in the tumor tissues of STYK1 deletion mice compared to WT mice. In order to study the mechanism of STYK1 in NK, RNA sequence of STYK1$^{-/-}$ and WT NK have unveiled a disparity in the signaling pathways linked to migration and adhesion in STYK1$^{-/-}$ NK cells. Further analysis of chemokine receptors associated with NK cell migration revealed that STYK1-deficient NK cells exhibited a significant reduction in CCR2 expression. The STYK1 expression was negatively associated with tumor progression in glioma patients. Overall, our study found the expression of STYK1 in NK cell mediates NK cell anti-tumor response through regulating CCR2 and infiltrating into tumor tissue.

Keywords Serine/threonine/tyrosine kinase 1 (STYK1), Natural killer (NK) cells, Tumor infiltrating, CCR2, Progression

*Correspondence:
Zhongjun Dong
dongzj@mail.tsinghua.edu.cn
Juan Du
duj656@ccmu.edu.cn
[1]Beijing Tsinghua Changgung Hospital, School of Clinical Medicine, Tsinghua University, Beijing 102218, China
[2]Institute for Organ Transplant and Bionic Medicine, Tsinghua University, Beijing 102218, China
[3]Department of Allergy, The First Affiliated Hospital of Anhui Medical University and Institute of Clinical Immunology, Anhui Medical University, Hefei 230032, China
[4]Innovative Institute of Tumor Immunity and Medicine (ITIM), Hefei 230032, China
[5]Anhui Province Key Laboratory of Tumor Immune Microenvironment and Immunotherapy, Hefei 230032, China
[6]Inflammation and Immune Mediated Diseases Laboratory of Anhui Province, Anhui Medical University, Hefei 230032, China
[7]State Key Laboratory of Membrane Biology, School of Medicine and Institute for Immunology, Tsinghua University, Beijing 100084, China
[8]National Key Laboratory of Intelligent Tracking and Forecasting for Infectious Diseases, Beijing Ditan Hospital, Capital Medical University, Beijing 100015, China
[9]Beijing Institute of Infectious Diseases, Beijing 100015, China
[10]National Center for Infectious Diseases, Beijing Ditan Hospital, Capital Medical University, Beijing 100015, China
[11]Beijing Key Laboratory of Emerging Infectious Diseases, Institute of Infectious Diseases, Beijing 100015, China
[12]Beijing Ditan Hospital, Capital Medical University, Beijing 100015, China
[13]Tsinghua University, Medical Blvd. D328, Haidian District, Beijing 100086, China

Background

The human STYK1 (serine/threonine/tyrosine kinase 1) was initially cloned as a potential tyrosine receptor protein kinase in 2003. STYK1 is located on human chromosome 12p13 and consists of 11 exons [1]. The STYK1 molecule is comprised of a single transmembrane helix and an intracellular tyrosine kinase domain, but lacks the extracellular domain. Moreover, STYK1 also called Novel Oncogene with Kinase-domain (NOK), is a newly identified oncogenic protein that belongs to the receptor tyrosine kinase (RTK) family. RTKs are the largest class of enzyme-linked receptors, and the inhibitors of RTK have significantly enhanced the prognosis of cancer. STYK1 shares approximately 30% amino acid identity with members of the platelet-derived growth factor/fibroblast growth factor (PDGF/FGF) receptor superfamily [2]. STYK1 plays a crucial role in the induction of tumorigenesis and metastasis [3]. STYK1 has been suggested as a potential diagnostic marker or prognostic indicator for various cancers [4, 5]. Studies have observed that high expression of STYK1 in tumor cells of patients with acute leukemia [6, 7], ovarian cancer [8] and even in the early stages of lung cancer [9]. The involvement of STYK1 in tumor growth and metastasis indicates that STYK1 is a promising therapeutic target for cancer therapy.

As the most prevalent and dangerous type of brain tumor, glioma poses a significant threat to life due to its high aggressiveness and poor prognosis, particularly when classified as high grade. Consequently, research on brain gliomas has garnered increasing attention from scholars worldwide. The knockdown of STYK1 has been shown to inhibit the proliferation, migration, and invasion of human glioma cell lines (U87MG, U251, and LN229) in vitro, as well as to suppress the growth of xenografted tumors in nude mice [10]. Additionally, STYK1 transgenic mice develop a disease resembling Chronic Lymphocytic Leukemia, which consistently manifests within the bone marrow [11]. However, the effects of STYK1 knockout mice on tumor genesis and the role of STYK1 in the immune system remain poorly understood.

In this study, we analyzed 198 cases from the human glioma Chinese Glioma Genome Atlas (CGGA) database to investigate the role of STYK1 in glioma patients. However, we found that STYK1 plays an anti-tumor role and is negatively associated with both tumor grade and prognosis in glioma patients. To explore the mechanism behind this, we analyzed the expression of STYK1 in immune cells using the 2013 Immunological Genome Project database. Our analysis revealed that STYK1 was primarily expressed in NK cells. To further investigate the function of STYK1 in NK cells, we created a STYK1-deficient mice model ($STYK1^{-/-}$) using CRISPR/Cas9 gene technology. We conducted experiments using four tumor models ($ß2M^{-/-}$ cells, RMA-S, MMTV-PyMT, B16F10), and observed that STYK1 deletion promoted tumor progression. Additionally, we found that $STYK1^{-/-}$ NK cells had reduced accumulation at the tumor site compared to WT mice. Further analysis using RNA-seq and flow cytometry showed that STYK1 promoted NK cell migration probably through regulating C-C Motif Chemokine Receptor 2 (CCR2) receptor. Overall, we generated STYK1-deficient mice to investigate its function in tumor progression and demonstrated the role of STYK1 in tumor infiltrating NK cells through CCR2.

Results

STYK1−/− mice have normal number, development, and function of NK cells in spleen and bone marrow in the resting state

RTKs act as both receptors for growth factors and enzymes that catalyze the phosphorylation of downstream target proteins. RTKs contained epidermal growth factor receptors (EGFR), the platelet-derived growth factor receptors (PDGFR), fibroblast growth factor receptors (FGFR), vascular endothelial growth factor receptors (VEGFR), rearranged during transfection (RET), and STYK1. By analyzing the expression of RTKs in immune cells in the database of 2013 Immunological Genome Project, we found that STYK1 was principally expressed in NK cells (Fig. 1A). Therefore, we speculated that STYK1 might affect the functional changes of NK cells. We quantified the relative proportions of NK cell subsets based on NK1.1 and CD11b expression. NK cells were categorized into three developmental stages: $CD3^{-}CD122^{+}NK1.1^{-}CD11b^{-}$ NK progenitors (NKp), $CD3^{-}CD122^{+}NK1.1^{+}CD11b^{-}$ immature NK cells (iNK), and $CD3^{-}CD122^{+}NK1.1^{+}CD11b^{+}$ mature NK cells (mNK). NK cells are derived from bone marrow hematopoietic stem cells (HSCs) through a gradual process, including common lymphoid progenitor (CLP), NK progenitor (NKp), immature NK (iNK), and mature NK cells (mNK). Then we examined the mRNA expression level of STYK1 in three stages of NK development, and observed that the expression of STYK1 was consistent with the data in the Immunological Genome Project (Fig. 1B). Thus, we generated the STYK1-deleted B6 mouse using CRISPR/Cas9 technology, and STYK1 gene was effectively knocked out in deletion mice (Fig. 1C). We investigated the impact of STYK1 knockout on NK cells in the resting state. We found that there were no significant changes observed in the number of NK and NKT cells in the spleen and bone marrow of both WT and $STYK1^{-/-}$ mice (Fig. 1D). Flow cytometry assay revealed that WT and $STYK1^{-/-}$ mice had normal number of T ($CD3^{+}CD19^{-}$) and B cells ($CD3^{-}CD19^{+}$) in spleen and bone marrow (Fig. 1E). Additionally, we also evaluated this process through the expression level of CD27 and

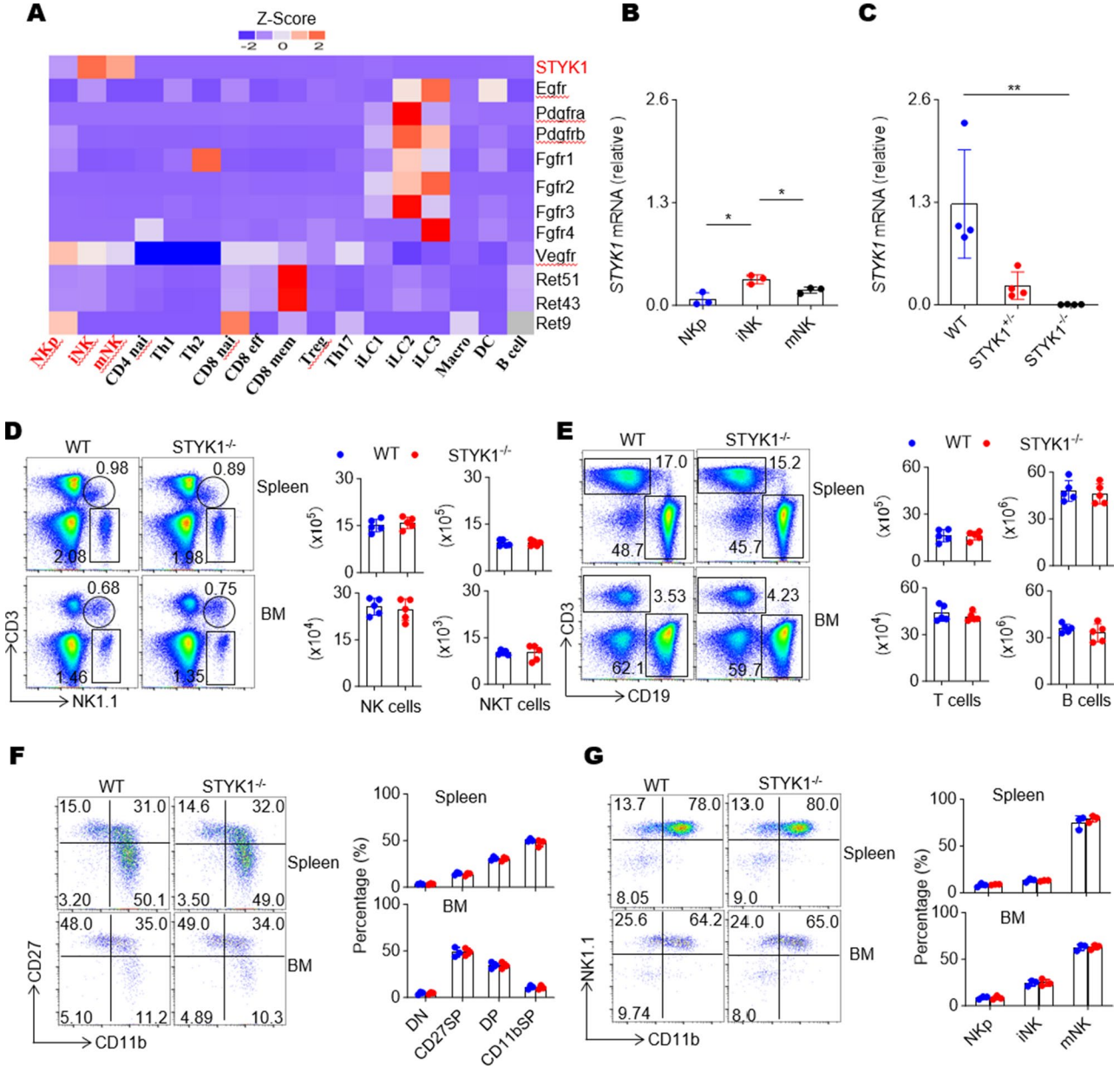

Fig. 1 STYK1$^{-/-}$ mice have normal number of T/B /NK cells in spleen and bone marrow at resting state. (**A**) The expression of STYK1 and other RTKs on immune cells in the database of 2013 Immunological Genome Project. (**B**) The mRNA expression of STYK1 on the development stage of NK cells from wildtype mice ($n=3$). (**C**) The mRNA expression of STYK1 on NK cells from STYK1 deficient and wildtype mice ($n=4$). (**D**-**E**) The number of NK (CD3$^-$NK1.1$^+$), NKT (CD3$^+$NK1.1$^+$), T (CD3$^+$CD19$^-$) and B (CD3$^-$CD19$^+$) cells in spleen and bone marrow was analyzed and calculated by flow cytometry. The representative data was on the left and the statistic date was on right ($n=5$). (**F**) Four-stage mature of NK cells, including CD27$^-$CD11b$^-$ (DN), CD27$^+$CD11b$^-$ (CD27 SP), CD27$^+$CD11b$^+$ (DP), and CD27$^-$CD11b$^+$ (CD11b SP) were gated on CD3$^-$CD19$^-$NK1.1$^+$ NK cells in the spleen and BM of WT and STYK1-deficient mice. The representative data was on the left and the statistic date was on right ($n=3$). (**G**) Early development of NK cells was defined by CD122, NK1.1 and CD11b, including NKp (CD3$^-$CD122$^+$NK1.1$^-$CD11b$^-$), iNK (CD3$^-$CD122$^+$NK1.1$^+$CD11b$^-$), mNK (CD3$^-$CD122$^+$NK1.1$^+$CD11b$^+$) in the spleen and BM of two mice group. The representative data was on the left and the statistic date was on right ($n=3$). The data are expressed as mean ± SD and represent one of three independent experiments. *, $P<0.05$; **, $P<0.01$; ***, $P<0.001$ by unpaired Student t tests (two-tailed)

CD11b by flow cytometry, we found that the NK cell maturation pattern defined by CD11b and CD27 between WT and STYK1 deficient mice were similar, indicating that STYK1 did not affect the NK cell maturation in spleen and bone marrow as shown in Fig. 1F. And flow cytometry assay also revealed that both the two kinds of mice had comparable development proportion of NKp (CD3$^-$CD122$^+$NK1.1$^-$CD11b$^-$), iNK (CD3$^-$CD122$^+$NK 1.1$^+$CD11b$^-$), and mNK (CD3$^-$CD122$^+$NK1.1$^+$CD11b$^+$) cells (Fig. 1G).

The primary functions of NK cells include the expression of CD107a and secretion of IFN-γ, which are

indicative of their ability to kill target cells and secrete cytokines. In vitro experiments of direct incubation NK cells with tumor cells can activate the expression of CD107a and secretion of IFN-γ. When stimulated by MHC-1 deficient tumor cells (YAC-1 or RMA–S), the IFN-γ secretion and CD107a expression were not influenced by STYK1 deficiency (Fig. 2A, B). When stimulated by cytokines such as IL-12, IL-18, and IL12 and IL-18, or antibody against NK1.1 or Ly49D, NK cells with or without STYK1 expression showed comparable IFN-γ secretion capability (Fig. 2C).

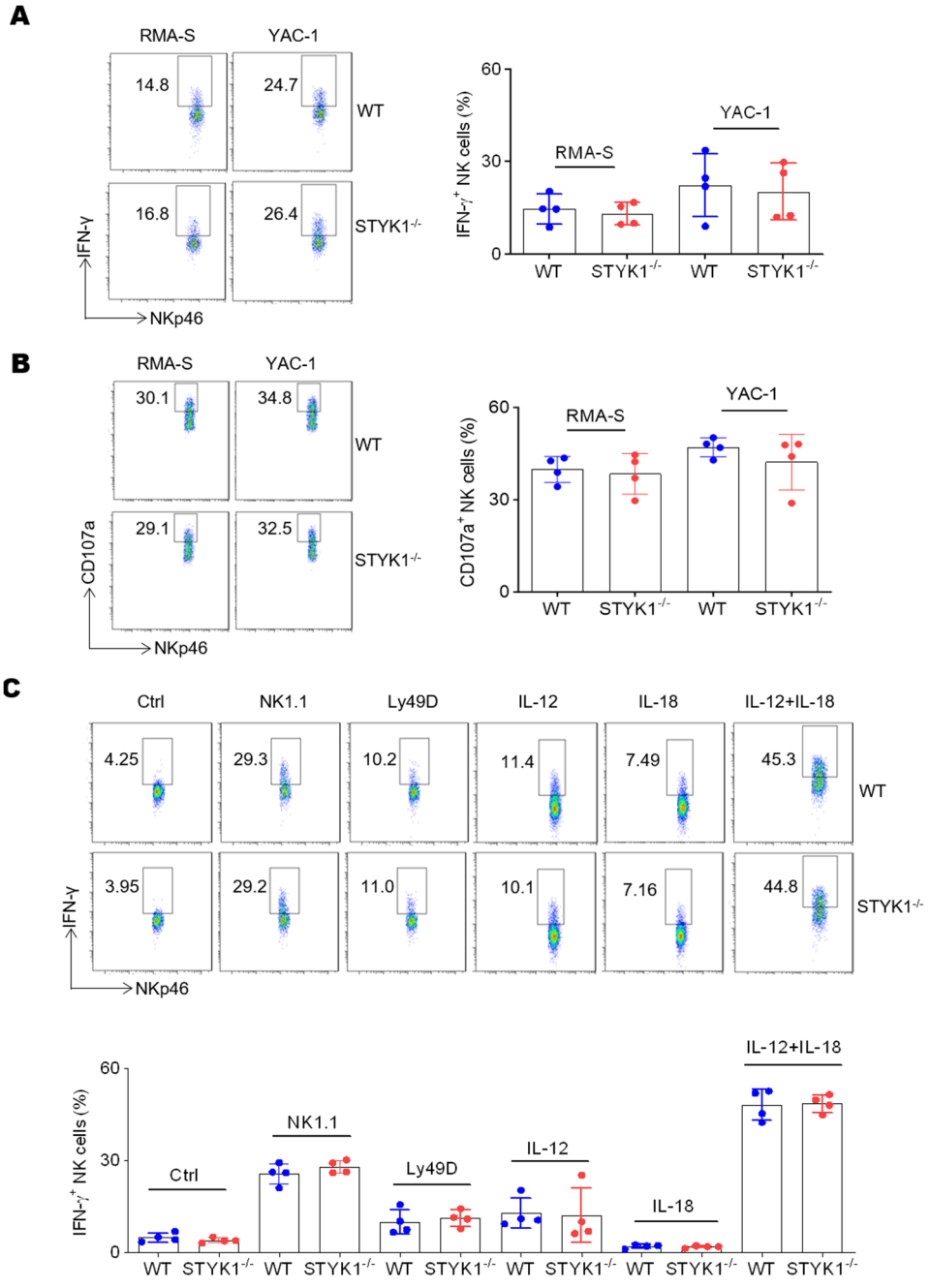

Fig. 2 NK cell function in STYK1 deletion mice at resting state. Polyl: C-activated splenocytes from WT and STYK1-deficient mice were incubated with the indicated target cells RMA-S and YAC-1. Expression of intracellular IFN-γ (**A**) ($n=4$) or CD107a (**B**) ($n=4$) by $CD3^{-}NKp46^{+}$ NK cells were analyzed. Polyl: C-activated splenocytes from WT and STYK1-deficient mice were stimulated by plate-coated antibody against IgG, NK1.1 or anti-Ly49D (10 mg/mL), and IL-12, IL-18, IL12 and IL-18 (10 mg/mL), isotype antibody was used as the control. Expression of intracellular IFN-γ (**C**) ($n=4$) by $CD3^{-}NKp46^{+}$ NK cells were analyzed. The data are expressed as mean ± SD and represent one of three independent experiments. *, $P<0.05$; **, $P<0.01$; ***, $P<0.001$ by unpaired Student t tests (two-tailed)

STYK1 deletion promotes B16F10 melanoma growth and metastasis through NK cells

To investigate the antitumor effect of STYK1 on NK cells, we conducted a transplantation tumor experiment using B16 melanoma cell line. Our findings revealed that tumor growth was significantly faster in knockout mice ($STYK1^{-/-}$) than in the control mice (WT) in subcutaneous injection model of B16 tumor cells ($p=0.023$), indicating that STYK1 functions as an anti-tumor function in the host immune system. As STYK1 was principally expressed in NK cells, so we hypothesize that STYK1 may influence NK cells. We found that the disparity in tumor growth between the two mouse types was eliminated after the depletion of NK cells using NK1.1 antibody, indicating that the difference in anti-tumor effect of knockout mice is mainly attributed to NK cells (Fig. 3A). Additionally, we isolated NK cells from mouse tumor tissue in B16 tumor model, and we detect the function of NK by NK1.1 and Ly49D antibody, target tumor cells YAC-1 and RMA-S, and IL12 and IL-18 in vitro. The CD107a expression of NK cells from tumor tissue was significantly inhibited by STYK1 deficiency by stimulating with NK1.1 and Ly49D antibody (Fig. 3B). The IFN-γ secretion of NK cells from tumor tissue was weakened by STYK1 deficiency by stimulating with NK1.1, but not Ly49D antibody and IL12 and IL-18 (Fig. 3C). When stimulated by YAC-1 and RMA-S, the CD107a expression of NK cells was significantly inhibited in deletion mice (Fig. 3D), and the IFN-γ secretion was inhibited by YAC-1(Fig. 3E). The CD107a expression and IFN-γ secretion of NK cells from tumor tissue was not influenced by STYK1 deficiency by stimulating IL12 and IL-18.

To further determine the anti-tumor function of STYK1, we conducted the lung metastasis tumor model using the tail vein injection of B16 melanoma cell line. We found that lung metastasis and weight was faster in knockout mice ($STYK1^{-/-}$) than in heterozygote deficient control mice ($STYK1^{+/-}$), further demonstrating that STYK1 functions as an anti-tumor function in the host immune system. Depletion of CD4 cells using CD4 antibody did not disturb the disparity in lung metastasis and weight between the two mouse types (Fig. 4A). Moreover, elimination of CD8 cells using CD8 antibody did not change the variation in lung metastasis and weight between the two mouse types (Fig. 4B). Only deletion of NK cells could eliminate disparity of the lung metastasis and weight between the knockout and control mice (Fig. 4C). Moreover, the number of NK cells in the lung was significantly decreased in STYK1-deficient mice (Fig. 4D). Overall, the anti-tumor immunity of STYK1-knockout mice might be attributed to NK cell in tumor tissue.

STYK1 deletion inhibit the elimination of NK target cells through diminishing NK cell number

To confirm the impaired function of NK cells in STYK1-deficient mice, we assessed the ability of NK cells to mediate "missing-self" rejection of MHC-I-missing splenocytes. The results showed that more than 90% of NK target cells were eliminated by NK cells in WT mice. However, NK cell-mediated killing was significantly reduced in STYK1-deficient mice (Fig. 5A). To further demonstrate tumor clearance in vivo, we investigated the role of NK cells in tumor clearance by injecting another NK cell target cells RMA-S. Equal proportions of GFP-labeled RMA-S cells and dsRed-labeled RMA-S cells were injected intraperitoneally into WT and $STYK1^{-/-}$ mice. Since NK cells can only deplete RMA-S cells lacking MHC-1 molecules, while RMA was used as a non-depleted control. The ability of STYK1 knockout NK cells to clear RMA-S cells was significantly reduced than in the wild-type mice (Fig. 5B). Peritoneal cell lavage fluid analysis showed that the NK cell percentage and number of STYK1-knockout mice was significantly lower than that of the control group (Fig. 5C), suggesting that the anti-tumor immunity of STYK1-knockout mice might be attributed to NK cells. While in the non-tumor model, the NK cell percentage and number in peritoneal cell lavage fluid from the knockout and WT mice model was almost the same (Fig. 5D).

STYK1 deficiency promotes spontaneous breast tumor progression by impairing NK cell accumulation in the tumor microenvironment

Then we investigated tumor progression in the spontaneous breast cancer mouse model (MMTV-PyMT), which realistically simulates the entire human tumor process. We crossed $STYK1^{-/-}$ mice with MMTV-PyMT mice and intercrossed the pups to generate female $STYK1^{-/-}$ MMTV-PyMT and $STYK1^{+/-}$ or $STYK1^{+/+}$ MMTV-PyMT control mice. Our study revealed that STYK1 deficient mice showed an increased severity of primary breast tumor and lung metastasis, as indicated by Fig. 6A-C. However, when we conducted in vitro culture of primary breast tumor-derived cells with varying genotypes ($STYK1^{+/+}$MMTV-PyMT, $STYK1^{+/-}$MMTV-PyMT, and $STYK1^{-/-}$MMTV-PyMT), we observed that tumor cells of all genotypes exhibited a similar growth rate, as illustrated in Fig. 6D. These results suggested that STYK1 might contribute to the progression and spread of breast tumors, regardless of the tumor cells characteristics. The results in the NK cell targets above led us to hypothesize that STYK1 in their mouse model may be related to abnormalities in STYK1-deleted NK cells. The PyMT tumor model revealed that STYK1 mice exhibited a significant reduction in the number of NK cells present in the tumor sites when compared to their WT

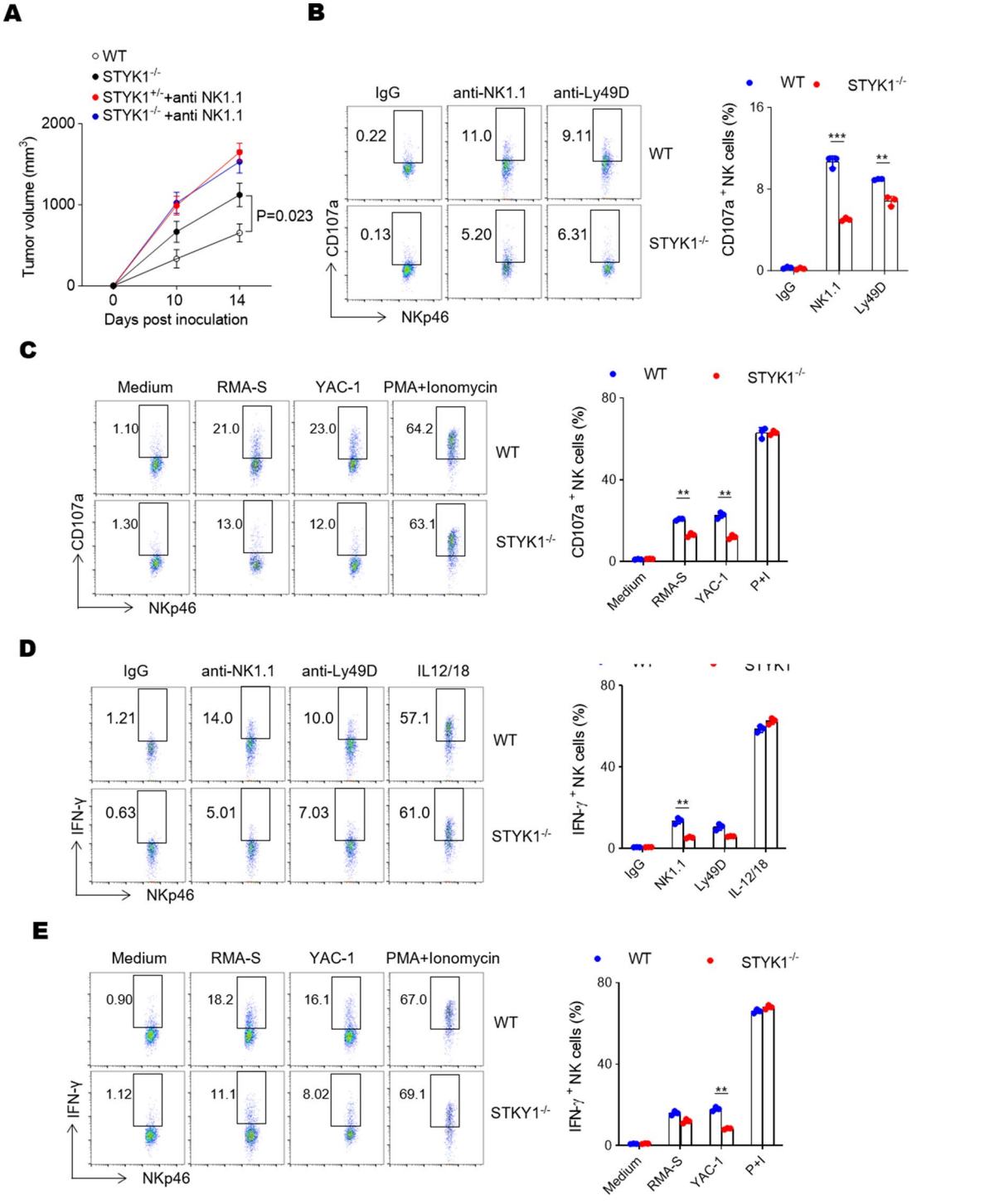

Fig. 3 The effect of STYK1 knockout mouse NK cells on B16 tumor growth. (**A**) 2×10^5 B16-F10 cells were injected subcutaneously into knockout mice ($STYK1^{-/-}$) and heterozygote deficient control mice ($STYK1^{+/-}$) each mouse ($n=4$), and the tumor size was measured between 10 and 14 days. (**B**-**E**) NK cells from the B16 bearing $STYK1^{+/-}$ and $STYK1^{-/-}$ mice were incubated with the indicated target cells, anti-NK1.1, anti-Ly49D antibody and IL12 and IL-18. Expression of intracellular CD107a (**B**, **C**) or IFN-γ (**D**, **E**) by $CD3^{-}NKp46^{+}$ NK cells were analyzed ($n=3$). The data are expressed as mean ± SD and represent one of three independent experiments. *, $P<0.05$; **, $P<0.01$; ***, $P<0.001$ by unpaired Student t tests (two-tailed)

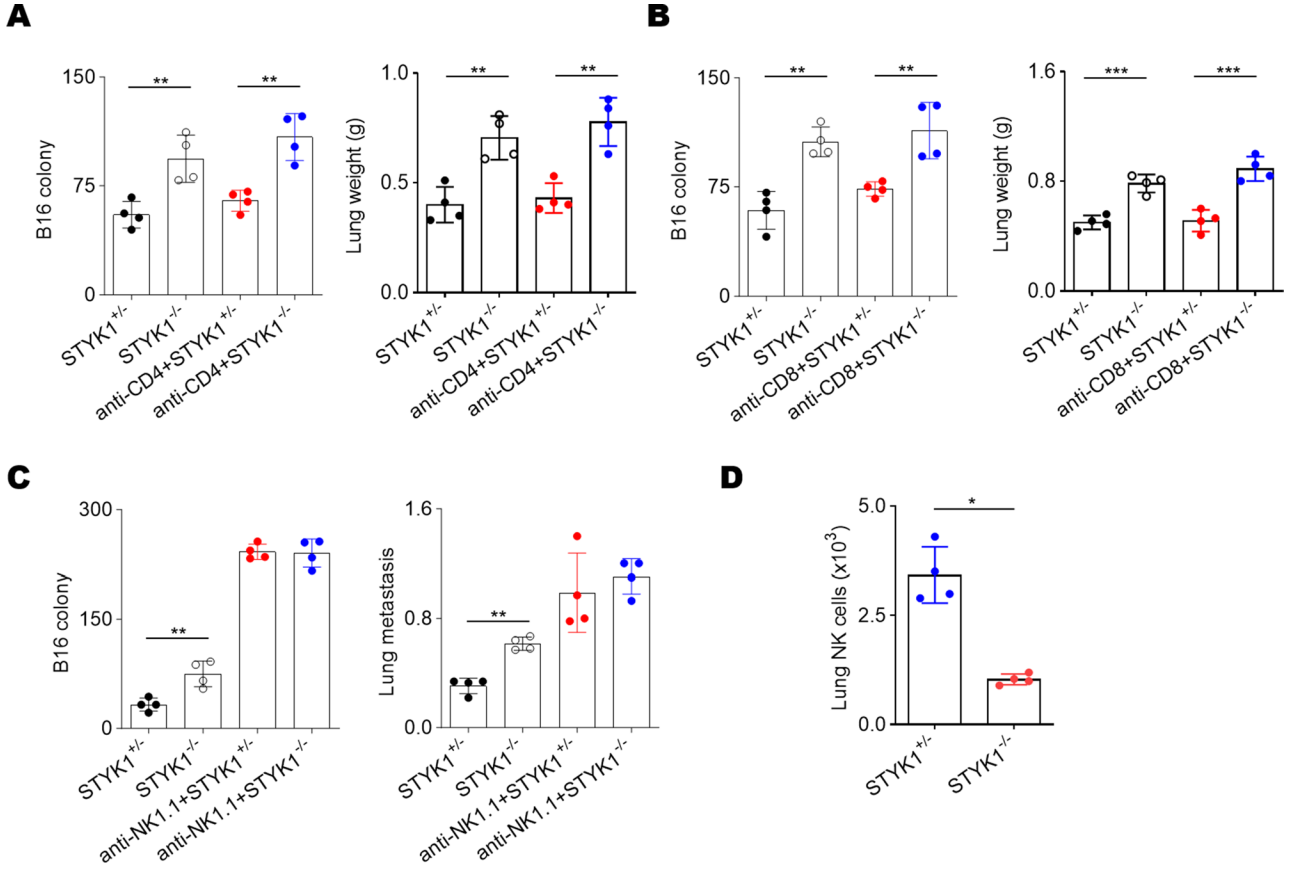

Fig. 4 The effect of STYK1 knockout mouse NK cells on B16 lung metastasis. 2×10^5 B16-F10 cells were injected into vein to induce lung metastasis. After a period of 14 days, the mice were sacrificed and the number of metastatic nodules and lung weights were counted. The $CD4^+$ T (**A**), $CD8^+$ T (**B**) and NK (**C**) cells from indicated mice were depleted by CD4 ($n=4$), CD8 ($n=4$), and NK1.1 antibody ($n=4$). Each symbol in the study represented a mouse. The P values were calculated using an unpaired T-test. (**D**) The number of NK from the lung of indicated mice was determined by flow cytometer ($n=4$). The data are expressed as mean ± SD and represent one of three independent experiments. *, $P<0.05$; **, $P<0.01$; ***, $P<0.001$ by unpaired Student t tests (two-tailed)

control mice. However, in the spleen, both the WT and $STYK1^{-/-}$ mice displayed a similar percentage of NK cells (Fig. 6E).

STYK1 promotes NK cell migration through the CCR2 receptor

In order to study the anti-tumor mechanism of STYK1 in NK, we isolated knockout $STYK1^{-/-}$ and control WT NK cells. We used RNA sequence method to study the altered signaling pathway in STYK1deletion. Our findings revealed a significant difference in signaling pathways associated with migration and adhesion in STYK1-deficient NK cells in knockout mice (Fig. 7A). These results were consistent with the reduced number of local NK cells observed in the tumor model above. Further analysis of chemokine receptors associated with NK cell migration revealed that STYK1-deficient NK cells exhibited a significant reduction in CCR2 expression (Fig. 7B). In vitro transwell migration assays demonstrated that the migration ability of STYK1-deficient NK cells to the CCR2 ligand, C-C Motif Chemokine Ligand 2 (CCL2), was significantly weakened, indicating that STYK1 plays a direct role in regulating NK cell migration (Fig. 7C). To confirm the sequencing results, we used flow cytometry to examine the expression of CCR2 in NK cells. Our findings showed a significant reduction in the expression of CCR2 in the NK cells of the spleen (Fig. 7D) and lung (Fig. 7E) of knockout mice in the tumor-bearing model as compared to the WT mice, which is consistent with the sequencing results. Additionally, the migration ability of STYK1-deficient NK cells to the CCR3 ligand, CCL11 and a CCR5 ligand CCL5, was not weakened (Fig. 7F, I). Moreover, we found no significant reduction in the expression of CCR3 and CCR5 in the NK cells of the spleen and lung of knockout mice in the tumor-bearing model as compared to the WT mice (Fig. 7G, H, J, K). Overall, STYK1 promotes NK cell migration through the CCR2 receptor.

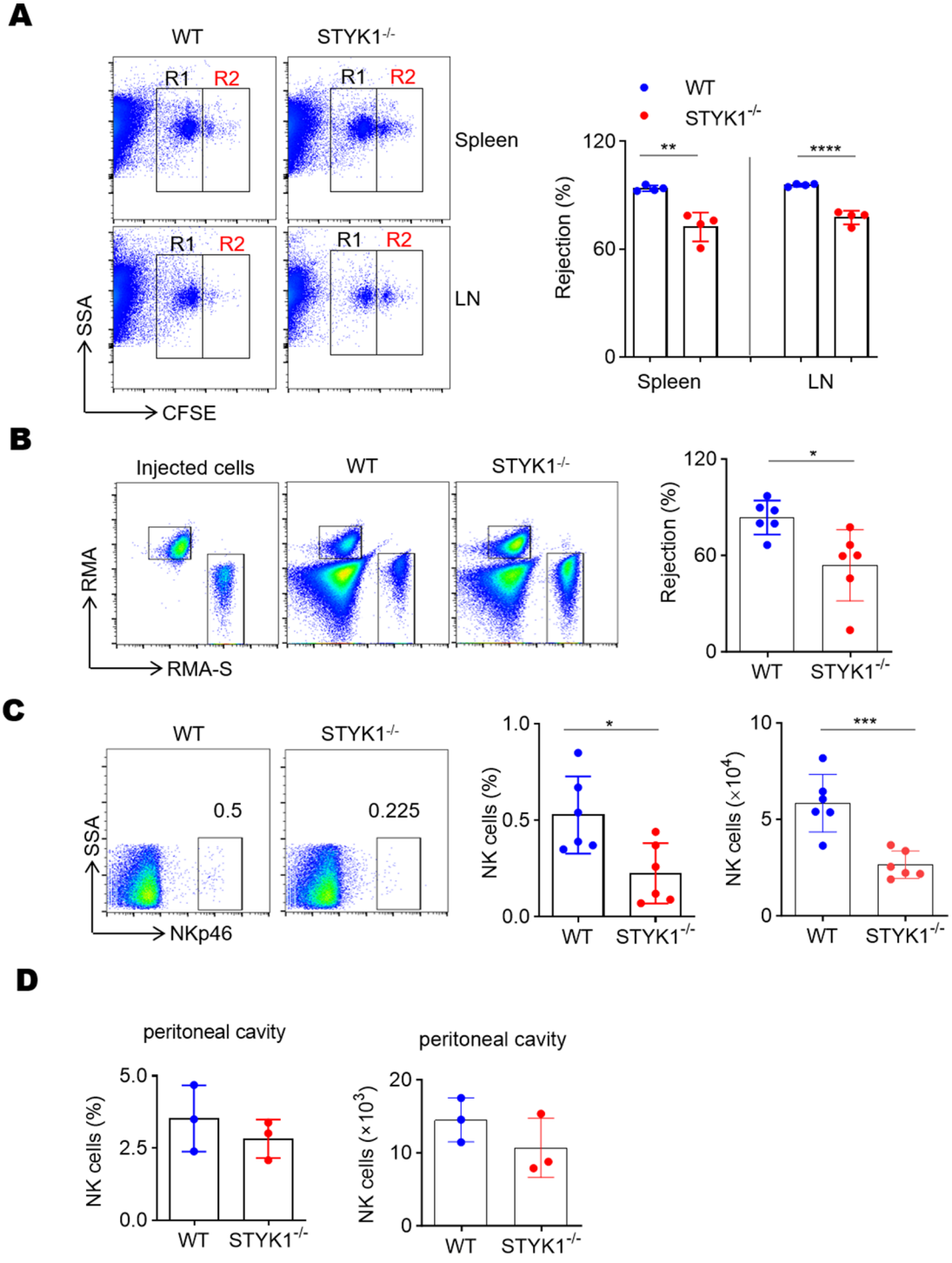

Fig. 5 STYK1 knockout inhibit the in vivo rejection of NK target tumor cells and the trafficking of NK cells to tumor site. (**A**) Representative flow cytometry plot of CFSE$^+$ cells obtained from the spleen and Lymph nodes (LN) of the indicated recipient mice at 18 h after injection with an equal number of C57BL/6 and ß2M-deficient splenocytes labeled with various concentrations of the cytosolic dye CFSE. R1, CFSE-low splenocytes from C57BL/6 mice; and R2, CFSE-high splenocytes from ß2M-deficient mice ($n=4$). (**B**) Equal number of NK cell-sensitive RMA-S cells expressing GFP and NK cell-resistant RMA cells expressing the fluorescent protein Ds-Red were intraperitoneally injected to the WT and STYK1 deletion mice. Left: representative flow cytometry plot of injected RMA-S cells in the peritoneal cavity at 18 h after injection. Right: the percentage of rejected RMA-S cells ($n=6$). (**C**) The percentage and the number of NK ($CD3^-NK1.1^+$) cells in peritoneal lavage fluids from the injected RMA-S mice model was analyzed by flow cytometry ($n=6$). (**D**) The percentage and the number of NK ($CD3^-NK1.1^+$) cells in peritoneal lavage fluids from the non-injected control mice was analyzed by flow cytometry ($n=3$). The data are expressed as mean ± SD and represent one of three independent experiments. *, $P<0.05$; **, $P<0.01$; ***, $P<0.001$ by unpaired Student t tests (two-tailed)

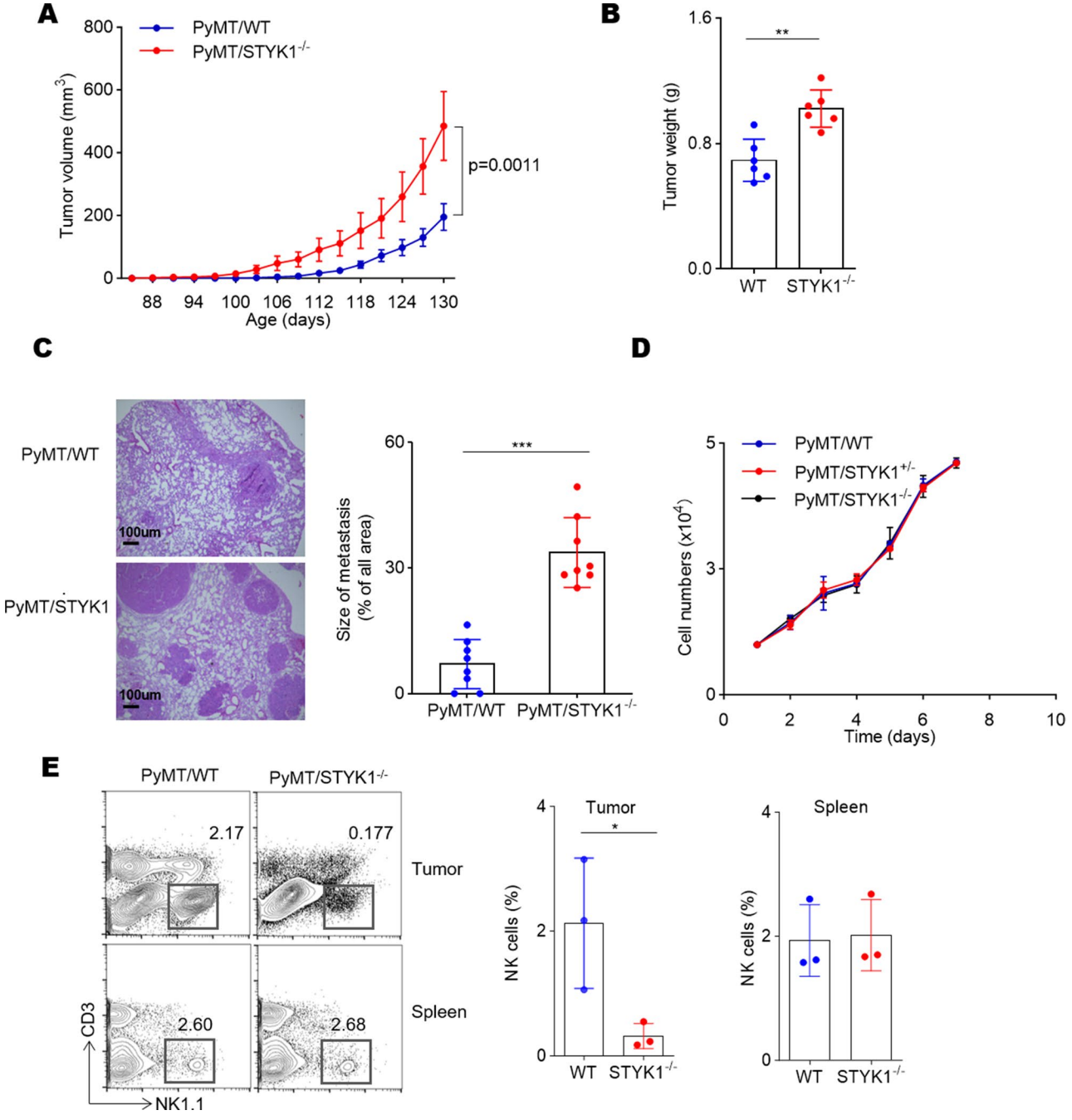

Fig. 6 STYK1 deletion promotes PyMT induced spontaneous breast tumor progression. (**A**) Mouse breast tumor sizes were measured by vernier caliper at the age of 12 weeks, once every three days, and ended by 19 weeks ($n=7$). (**B**) The tumor weight of the breast tumor was detected at 19 weeks ($n=6$). (** $p<0.01$). (**C**) The lung metastasis of spontaneous breast tumor was detected by hematoxylin eosin (H&E) staining ($n=7$). (*** $p<0.001$). (**D**) Primary breast tumors from *STYK1* WT MMTV-PyMT, *STYK1*$^{+/-}$ MMTV-PyMT, and *STYK1*$^{-/-}$ MMTV-PyMT mice were collected and digested by collagenase I (1 mg/ml). The single primary breast tumor cells were cultured in Dulbecco's Modified Eagle Medium (DMEM) supplemented by 10% fetal bovine serum (FBS) ($n=3$). (**E**) The percentage of NK cells in breast tumor microenvironment and spleen were analyzed by flow cytometry ($n=3$). The data are expressed as mean ± SD and represent one of three independent experiments. *, $P<0.05$; **, $P<0.01$; ***, $P<0.001$ by unpaired Student t tests (two-tailed)

STYK1 expression level was negatively correlated with the prognosis and grade of glioma patients

Our group has been paying special attention to glioma survival. To investigate the impact of STYK1 on tumor progression in real world study, we analyzed 198 cases from the human glioma CGGA database. We found that as tumor grade increases, the expression of STYK1 decreases significantly (Fig. 8A). Analysis of data from full-grade glioma patients revealed that individuals with high expression of STYK1 in tumor tissues had

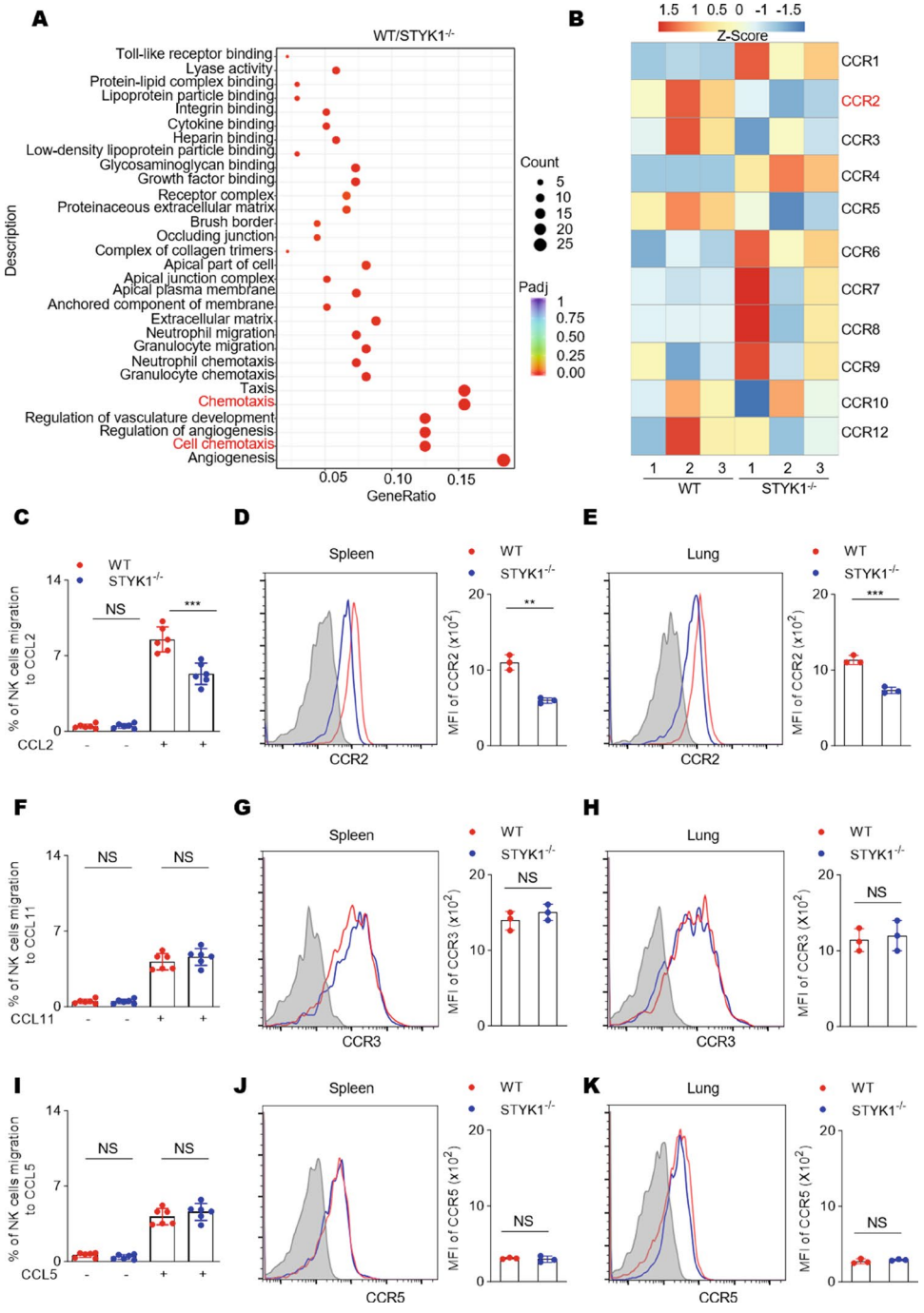

Fig. 7 STYK1 promotes NK cell migration through the CCR2 receptor. (**A**) Spleen NK cells were isolated from both STYK1$^{-/-}$ and wild-type mice, and then were sorted for transcriptomic sequencing. Gene function enrichment analysis was then performed. (**B**) RNA sequencing revealed the expression of the chemokine receptor family in STYK1 knockout and WT mice ($n=3$). (**C**) NK cells were cultured with CCL2 in a transwell chamber. After 12 h, the percentage of NK cells migrated towards CCL2 was calculated ($n=6$). (**D**, **E**) 2×10^5 B16-F10 cells were injected into vein to induce lung metastasis. After a period of 14 days, the mice were sacrificed. Flow cytometry was used to detect the CCR2 expression of NK cell in spleen and lung of the model ($n=3$). (**F**) NK cells were cultured with CCL11 in a transwell chamber. After 12 h, the percentage of NK cells migrated towards CCL11 was calculated ($n=6$). (**G**, **H**) 2×10^5 B16-F10 cells were injected into vein to induce lung metastasis. After a period of 14 days, the mice were sacrificed. Flow cytometry was used to detect the CCR3 expression of NK cell in spleen and lung of the model ($n=3$). (**I**) NK cells were cultured with CCL5 in a transwell chamber. After 12 h, the percentage of NK cells migrated towards CCL5 was calculated ($n=6$). (**J**, **K**) 2×105 B16-F10 cells were injected into vein to induce lung metastasis. After a period of 14 days, the mice were sacrificed. Flow cytometry was used to detect the CCR5 expression of NK cell in spleen and lung of the model ($n=3$). (** $p<0.01$, *** $p<0.001$). The data are expressed as mean ± SD and represent one of three independent experiments. *, $P<0.05$; **, $P<0.01$; ***, $P<0.001$ by unpaired Student t tests (two-tailed)

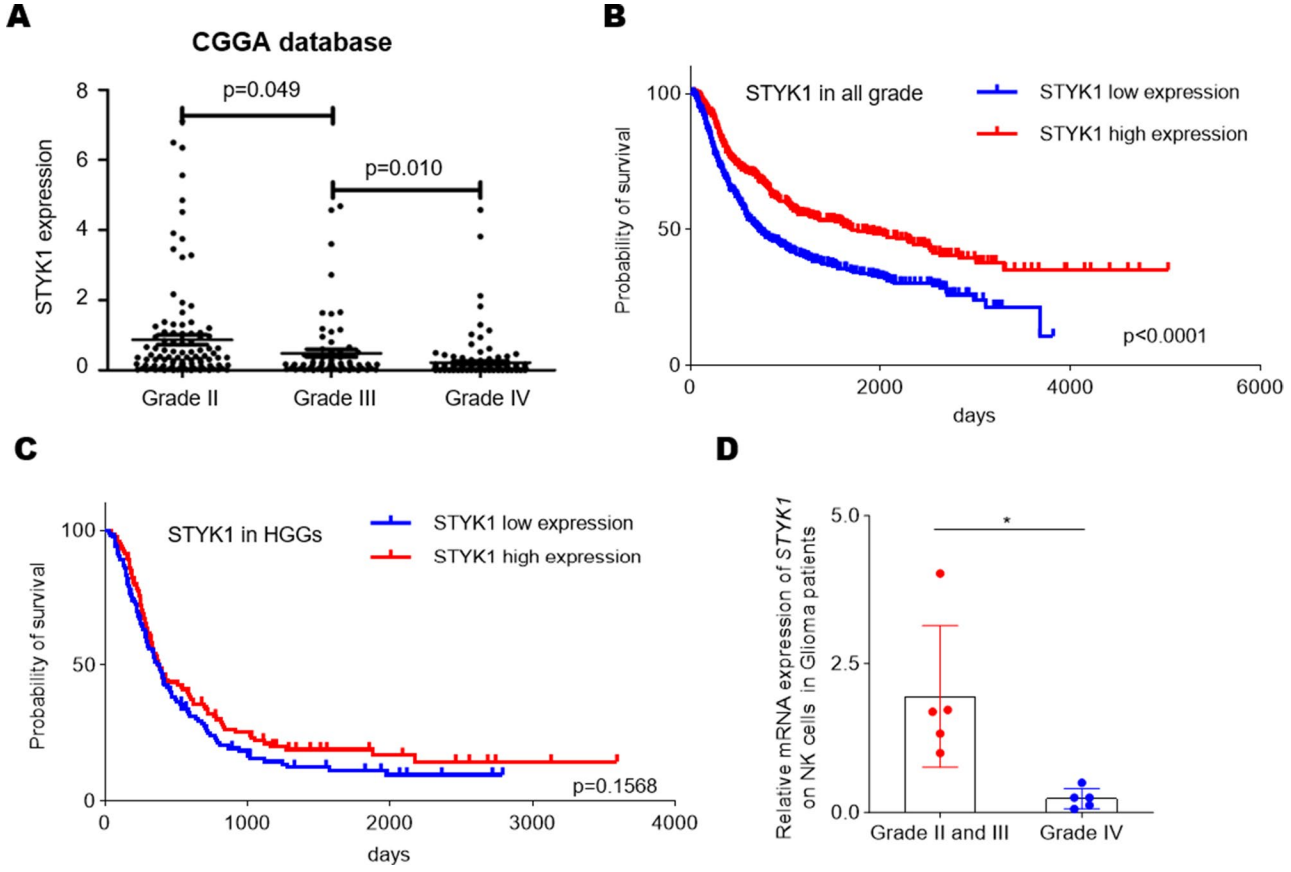

Fig. 8 STYK1 expression level was negatively correlated with the prognosis and grade of glioma patients. (**A**) The correlation between STYK1 expression and glioma grade and prognosis were analyzed using the glioma CGGA chip database. The results showed a gradual increase in malignancy with higher glioma grades (II, III, and IV). (**B**-**C**) The relationship between STYK1 expression and patient prognosis in those with full-grade and more malignant glioma ($n=6$). The grade IV glioma was also called high grade glioma (HGG). (**D**)The mRNA expression level of STYK1 in NK cells from the low-grade patients was significantly decreased than that from the high-grade glioma patients ($n=5$). The data are expressed as mean ± SD and represent one of three independent experiments. *, $P<0.05$; **, $P<0.01$; ***, $P<0.001$ by unpaired Student t tests (two-tailed)

a significantly better prognosis ($p<0.0001$, Fig. 8B). While analysis of data from high grade glioma (HGG) revealed that individuals with high expression of STYK1 in tumor tissues had a slightly better prognosis, but not significant ($p=0.1568$, Fig. 8C). The in vivo evidence suggests that STYK1 plays an anti-tumor role in glioma patients. To verify that the anti-tumor effect was due to NK cells, we isolate NK cells from tumor tissues of five low-grade (Grade II+III) and five high-grade (Grade IV) glioma patients. The mRNA expression level of STYK1 in NK cells from the low-grade patients was significantly decreased than that from the high-grade glioma patients (Fig. 8D). Overall, the STYK1 expression was negatively associated with tumor progression in glioma patients.

Discussion

NK cells play a crucial role in providing initial immune protection against malignancies [12], and several immunotherapies based on NK cells have been suggested for treating human cancer [13]. Restoring NK cell function by overcoming the immunosuppressive tumor microenvironment is a promising therapeutic approach. Despite the clinical potential of NK cells, several limitations currently exist that naturally hinder the effective use of NK cells in cancer therapy, including NK cell effector functions, tumor resistance, and infiltration to tumor [14]. The infiltration of NK cells into tumor tissues and their close contact with tumor cells are crucial for an effective anti-tumor response. Previous studies have shown that the presence of cytotoxic NK cells in tumor infiltration is associated with better prognosis in various types of cancer [15], including breast cancer [16], non-small cell lung carcinomas [17, 18], colorectal cancer [19], gastric carcinoma [20], and renal cell carcinomas [21]. However, there is also evidence suggesting that in the initial stage of tumor, the infiltration of NK cells into tumor tissues is impaired, which is inversely correlated with prognosis or the efficacy of NK cell therapy [22]. For instance, a clinical study on colorectal cancer analyzed the localization and densities of NK cells in primary tumor tissue, liver

metastases, adenomas, and normal tissue sections from 112 patients, and revealed that NK cells were generally absent in tumor tissue at all stages, while in adjacent normal mucosa, the numbers of NKp46$^+$ NK cells were significantly higher than those in primary tumor tissue [19]. Further understanding of how NK cells infiltrate tumor sites is crucial for overcoming the challenges associated with NK cell therapy in cancer treatment.

Our study analyzed the of expression RTKs in immune cells of 2013 Immunological Genome Project, and found that STYK1 was principally expressed in NK cells. We discovered that STYK1 deletion mice have normal number, development, and function of NK cells in tumor-free resting state. These data were consistent with the Thierry Walzer lab in that we both found that STYK1 deficient NK cells develop normally and have normal in vitro and in vivo effector functions [23]. But we performed tumor burden experiments with four tumor model on STYK1 knockout and control mice, we found that the ability of STYK1 deletion mice to eliminate tumor cells was significantly reduced. We observed a reduction of NK cell accumulation in the tumor tissues of STYK1 deletion mice, and this decrease might be due to the reduced expression of chemokine receptor CCR2. Therefore, we provide a promising strategy to improve the homing and infiltration into tumors of NK cells by promoting STYK1/CCR2 signaling.

As a member of the receptor tyrosine kinase family, STYK1 has traditionally been regarded as an oncogene in various tumors. In glioma, the knockdown of STYK1 inhibits proliferation, migration, and invasion in human glioma cell lines such as U87MG, U251, and LN229 in vitro [10]. However, the role of STYK1 knockout on tumor growth in vivo remains unclear. Although STYK1 transgenic mice exhibit a disorder similar to Chronic Lymphocytic Leukemia [11], the effects of overexpression and knockout are in consistent and vary among different tumor types. Therefore, we employed knockout mice in this study to investigate the impact of STYK1 on tumor growth in vivo. Additionally, the use of tyrosine kinase inhibitors (TKI) has significantly enhanced the prognosis of cancer [24]. However, despite their effectiveness, TKI cannot be deemed curative therapeutic agents, as most patients develop resistance or do not achieve complete molecular remission [25]. Furthermore, patients who undergo life-long treatment may encounter adverse effects that adversely affect their quality of life [26]. For the clinical trials, the European stop tyrosine kinase inhibitor study (EURO-SKI), and clinical evidences indicated that patient's immune system may play a key role in preventing relapses [27]. Notably, TKI may impair hematopoiesis, consequent to the inhibitory effect on c-KIT transduction and Src kinase pathway [28]. Reports had also showed that TKI exert an inhibitory effect on NK cells, sharply inhibited the cytotoxic NK cells [29]. Our study provides a mechanism for the limited effect of TKIs on tumors, that TKI inhibitors might restrain the infiltration of NK cells to tumors by inhibiting STYK1 function.

In conclusion, we have determined that mice with a deletion of the STYK1 gene exhibit a normal count, development, and functionality of natural killer (NK) cells in both the spleen and bone marrow during a resting state without any tumors present. Additionally, we have uncovered that the removal of STYK1 gene promotes the progression of tumors, leading to a decrease in the accumulation of NK cells within the tumor tissues of the STYK1 deletion mice. Our further analysis focused on chemokine receptors that are involved in the migration of NK cells, revealing that STYK1-deficient NK cells display a significant decline in the expression of CCR2, which is a critical receptor for their tumor infiltration. Furthermore, we have observed a negative correlation between the expression of STYK1 and the advancement of glioma tumors in patients. Overall, our study provides evidence that the expression of STYK1 within NK cells is essential for their anti-tumor response by regulating CCR2 and facilitating their infiltration into tumor tissues.

Materials and methods

Mice

STYK1$^{-/-}$ mice were generated by standard CRISPR/Cas9 gene technology on C57BL/6 background in our lab, and Exons 1 and 2 of STYK1 gene were knocked out. The founder mice were identified by genomic PCR at three weeks of birth using the following pairs of primers: STYK1F 5'-GTCTTTGGAAATACTGCACC-3', STYK1R 5'-GTTTGAGCCTTACCTCGGGGTC-3'. The PCR products were obtained after denaturation at 94 C for 5 min, and followed by amplifing for 35 cycles at a condition of 94° for 30s, 57° for 30s, 72° for 45s. PyMT mice transgenic mice was from Jackson Laboratory and backcrossed on C57BL/6 background at least 12 generations. PyMT male offspring was mated with *STYK1*$^{-/-}$ mice to generate the PyMT/*STYK1*$^{+/-}$, and further mated with *STYK1*$^{+/-}$ to generate PyMT/WT and PyMT/*STYK1*$^{-/-}$ mice. All the mice were C57BL/6 background and maintained under specific pathogen-free animal facilities. All procedures of animals were approved by the Animal Ethics Committee.

For the subcutaneous tumor model, B16F10 melanoma cells were resuspended in 1×PBS and subcutaneously injected into the mice (2×10^5 cells/mouse). After that, tumor volume was assessed every 3 days by measuring the length and width of individual tumors with a caliper. Fourteen days later, the mice were sacrificed and in vitro NK-cell function of tumor tissues were assayed. For the lung metastasis mouse model, B16F10 melanoma cells were resuspended in 1×PBS and intravenously injected

into the mice (2×10^5 cells/mouse). Fourteen days later, the mice were sacrificed. The lung was weighed and the number of lung surface nodules was counted under a dissecting microscope. The function of NK cells of the lung were defined in vitro.

Only female mice were used for the PyMT model, because the incidence of tumors in male was significantly decreased than female mic. Tumor volume was assessed every 3 days by measuring the length and width of individual tumors with a caliper. The volume of each tumor was approximated as the volume of an oblong spheroid of the measured length (l) and width (w), that is V (tumor)=πlw2/6. The individual tumor volumes were summed to give the total tumor volume in each mouse. The mice were killed when tumors reached a maximum size of 2 cm^3. For histological examination of the metastases, lungs were fixed in 4% paraformaldehyde, embedded in paraffin, sectioned, stained with H&E and scanned by light microscopy for metastatic foci. Photomicrographs of H&E-stained slides of lung metastases were analyzed with the Image J software (Bethesda, MD, USA) to assay the metastatic surface/lung.

Flow cytometry

Splenocytes from the indicated mice were resuspended in PBS buffer containing 2% fetal bovine serum, and were incubated surface antibodies for 30 min at 4 °C. Then cells were fixed and permeabilized using Cytofix/Cytoperm reagent (BD Biosciences). The intracellular antibodies were stained and analyzed by flow cytometry. Monoclonal antibodies against mouse CD3e (eBio500A2), NK1.1 (PK136), CD19 (1D3), CD11b (M1/70), CD27 (LG.7F9), CD122 (TMbetal), NKp46 (29A1.4), IFN-γ(XMG1.2), CD107a (eBio1D4B), CCR2 (475301), CCR3 (J073E5), CCR5 (7A4), and isotype controls were purchased from eBioscience (San Diego, CA) or BD Biosciences (Mississauga, Ontario, Canada). The expression level was presented as relative ratio or net mean fluorescence intensity, which was determined by subtracting the mean fluorescence intensity of isotype control.

In vitro NK-cell function assays

Poly(I: C)-activated splenocytes were co-cultured with NK-sensitive tumor cells YAC-1 and RMA-S in the presence of anti-CD107a (clone eBio1D4B). Splenocytes stimulated with PMA (50 ng/mL) plus ionomycin (1 μM) stimulation were used as positive controls. For antibody stimulation, purified anti-NK1.1 and Ly49D at the concentration of 1 μg/mL were pre-coated on the 24-well plate overnight at 4 °C before adding splenocytes. For cytokine stimulation, recombinant mouse IL-12 (10 ng/mL) and recombinant mouse IL-18 (10 ng/mL) were added to the splenocytes. After co-culturing with GolgiStop (BD, Biosciences) for 6 h, cells were harvested and stained with the indicated antibodies, fixed, permeabilized, and then stained with an anti-IFN-γ antibody.

In vivo β2M-deficient splenocytes rejection assay

Splenocytes obtained from the mice lacking β2M were processed to remove red blood cells using Ficoll density gradient centrifugation. These splenocytes were then labeled with a fluorochrome dye called CFSE at a concentration of 5 μM. In parallel, splenocytes from C57BL/6 mice were also labeled with CFSE, but at a much lower concentration of 0.5 μM (10 times less than the β2M cells). Both types of CFSE-labeled splenocytes were mixed in equal proportions (1:1 ratio). This mixture, containing a total of 2×10^6 splenocytes, was injected intravenously into mice that had been pretreated with 200 μg of Poly (I: C). After eighteen hours, flow cytometry was used to assess the presence of CFSE-positive cells in the spleen and lymph nodes. The percentage of β2M-deficient splenocytes rejection was calculated as following: 100 × [1 − (percentage of residual β2M-deficient splenocytes in total $CFSE^+$ cell/percentage of β2M-deficient splenocytes in total injected $CFSE^+$ cell)].

In vivo RMA-S clearance assay

In this experiment, mice were treated with Poly (I: C) at a concentration of 200 μg for 18 h. Afterwards, a mixture of tumor cells and NK-sensitive cells (RMA-S-GFP) as well as NK-non-sensitive cells (RMA-Ds-Red) were mixed at a 1:1 ratio, and injected intraperitoneally into the indicated mice. After another 18 h, the mice were sacrificed, and the cells in the peritoneal cavity were collected through repeated washing with PBS containing 2 μM EDTA. The flow cytometry was then used to determine the relative percentage of remaining RMA-S-GFP and RMA-Ds-Red cells. The percentage of RMA-S cell rejection was calculated as below: 100 × [1 − (percentage of the residual GFP^+ population among the total GFP^+ and Ds-Red^+ cells/percentage of the total GFP^+ population among the total GFP^+ and Ds-Red^+ cells)].

Cell growth curve of PyMT tumor cells

For the cell growth assay, PyMT tumor cells (1×10^4) from the PyMT/WT, PyMT/$STYK1^{+/-}$, and PyMT/$STYK1^{-/-}$ mice were seeded in triplicate in 35-mm wells for 24 h. The number was counted by a C6 flow cytometer every 24 h for 7 days (BD Biosciences, Becton Dickinson, Mountain View, CA, USA).

RNA sequencing of NK cells

Splenic NK cells were sorted on BD FACS AriaII (BD Biosciences) from $STYK1^{-/-}$ and WT control mice. Total RNA was extracted using the RNeasy Micro Kit (Qiagen, 74004) according to the manufacturer's instructions. RNA purity and quantification were then assessed with

a NanoDrop 2000 spectrophotometer (Thermo Scientific, USA), while RNA integrity was evaluated using the Agilent 2100 Bioanalyzer (Agilent Technologies, USA). Libraries were subsequently constructed using the Single Cell Full Length mRNA-Amplification Kit (Vazyme, N712-03, China) and the TruePrep DNA Library Prep Kit V2 for Illumina (Vazyme, TD502-02, China), following the manufacturer's guidelines. Transcriptome sequencing and analysis were performed by Annaroad Gene Technology Co., Ltd. (Beijing, China).

Reverse transcription PCR

Total RNA was extracted using the TRIZOL Kit (Invitrogen, Carlsbad, MA, USA), and reverse-transcribed using reverse transcription system (Promega, Madison, WI, USA). Quantitative PCR was performed using SYBR Green-based detection. Relative mRNA levels relative to the expression of β-actin were determined using the 2(−ΔΔCt) method. Three independent experiments were performed, with triplicate for each experiment. STYK1 Mouse qPCR Primer Pairs: Forward Sequence-5'ATCTCCTCTGCTCGATCCAGCA3', Reverse Sequence -'GAGTCACCATCTCATAAAGCAGG3'. STYK1 Human qPCR Primer Pair: Forward Sequence5'-CCATACCTCTCAAGTGGCTTGC3', Reverse Sequence 5'GAGTCACCATCTCATAGAGCAGG3'.

CGGA analysis of STYK1 expression and clinical characterizations of patients

STYK1 expression analyzed in 692 brain glioma samples, which is downloaded from CGGA including 188 grade II, 255 grade III, and 249 grade IV. Then, STYK1 expression profile and whole follow-up information are obtained from the CGGA RNA-seq set. The mean survival time for all 692 patients was 1199 days, approximately 3.28 years. Specifically, the mean survival time for the 188 grade II and 255 grade III patients were 1828 days and 1319 days, respectively, while the mean time for the 249 grade IV patients was only 616 days. Total points over 700 could predict a survival rate of less than 50% for 1-year survival, less than 20% for 2-year survival, and less than 10% for 3-year survival. Graphpad software was used for the statistics and drawing figures. Student's t test was performed to explore the expression distribution in different grade groups. We performed Kaplan-Meier analysis to explore the prognostic value of STYK1.

Statistical analyses

Statistical significance was determined using Prism software. Two-tailed unpaired or paired Student's t-tests between two groups and two-way analysis of variance (ANOVA) across multiple groups were used to determine significance. A p value of less than 0.05 was considered significant. $^{*}p<0.05$, $^{**}p<0.01$, $^{***}p<0.001$, $^{****}p<0.0001$.

Author contributions

JH performed the experiments and analyzed the data. YH, RB and YW performed the experiments and crossed the mice. ZD participated in the critical review of the manuscript and revised the manuscript. JD designed the experiments, analyzed the data and wrote the manuscript. All authors contributed to the article and approved the submitted version.

Funding

This work was supported by National Natural Science Foundation of China (81902895 and 82371565 to JD), Beijing Natural Science Foundation (M21007 to JD), and the China Postdoctoral Science Foundation (to JH, 2020M670296 and 2021T140372).

Data availability

All data needed to evaluate the conclusions in the paper are present in the paper or in the public database.

Declarations

Conflict of interest

The authors declare no conflict of interests.

Received: 10 June 2024 / Accepted: 1 October 2024
Published online: 16 October 2024

References

1. Ye X, Ji C, Huang Q, Cheng C, Tang R, Xu J, et al. Isolation and characterization of a human putative receptor protein kinase cDNA STYK1. Mol Biol Rep. 2003;30(2):91–6.
2. Liu L, Yu XZ, Li TS, Song LX, Chen PL, Suo TL, et al. A novel protein tyrosine kinase NOK that shares homology with platelet- derived growth factor/fibroblast growth factor receptors induces tumorigenesis and metastasis in nude mice. Cancer Res. 2004;64(10):3491–9.
3. Hu L, Chen HY, Cai J, Zhang Y, Qi CY, Gong H, et al. Serine threonine tyrosine kinase 1 is a potential prognostic marker in colorectal cancer. BMC Cancer. 2015;15:246.
4. Chen P, Li WM, Lu Q, Wang J, Yan XL, Zhang ZP, et al. Clinicopathologic features and prognostic implications of NOK/STYK1 protein expression in non-small cell lung cancer. BMC Cancer. 2014;14:402.
5. Chung S, Tamura K, Furihata M, Uemura M, Daigo Y, Nasu Y, et al. Overexpression of the potential kinase serine/ threonine/tyrosine kinase 1 (STYK 1) in castration-resistant prostate cancer. Cancer Sci. 2009;100(11):2109–14.
6. Kondoh T, Kobayashi D, Tsuji N, Kuribayashi K, Watanabe N. Overexpression of serine threonine tyrosine kinase 1/novel oncogene with kinase domain mRNA in patients with acute leukemia. Exp Hematol. 2009;37(7):824–30.
7. Nirasawa S, Kobayashi D, Kondoh T, Kuribayashi K, Tanaka M, Yanagihara N, et al. Significance of serine threonine tyrosine kinase 1 as a drug resistance factor and therapeutic predictor in acute leukemia. Int J Oncol. 2014;45(5):1867–74.
8. Jackson KA, Oprea G, Handy J, Kimbro KS. Aberrant STYK1 expression in ovarian cancer tissues and cell lines. J Ovarian Res. 2009;2(1):15.
9. Amachika T, Kobayashi D, Moriai R, Tsuji N, Watanabe N. Diagnostic relevance of overexpressed mRNA of novel oncogene with kinase-domain (NOK) in lung cancers. Lung Cancer. 2007;56(3):337–40.
10. Zhou J, Wang F, Liu B, Yang L, Wang X, Liu Y. Knockdown of serine threonine tyrosine kinase 1 (STYK1) inhibits the Migration and Tumorigenesis in Glioma cells. Oncol Res. 2017;25(6):931–7.
11. Yang Y, Liu L, Tucker HO. The malignant transformation potential of the oncogene STYK1/NOK at early lymphocyte development in transgenic mice. Biochem Biophys Rep. 2024;38:101709.
12. Myers JA, Miller JS. Exploring the NK cell platform for cancer immunotherapy. Nat Rev Clin Oncol. 2021;18(2):85–100.
13. Shimasaki N, Jain A, Campana D. NK cells for cancer immunotherapy. Nat Rev Drug Discov. 2020;19(3):200–18.
14. Tong L, Jiménez-Cortegana C, Tay A, Wickström S, Galluzzi L, Lundqvist A. NK cells and solid tumors: therapeutic potential and persisting obstacles. Mol Cancer. 2022;21(1):206.

15. Ran GH, Lin YQ, Tian L, Zhang T, Yan DM, Yu JH, et al. Natural killer cell homing and trafficking in tissues and tumors: from biology to application. Signal Transduct Target Ther. 2022;7(1):205.
16. Mamessier E, Sylvain A, Thibult ML, Houvenaeghel G, Jacquemier J, Castellano R, et al. Human breast cancer cells enhance self tolerance by promoting evasion from NK cell antitumor immunity. J Clin Invest. 2011;121(9):3609–22.
17. Platonova S, Cherfils-Vicini J, Damotte D, Crozet L, Vieillard V, Validire P, et al. Profound coordinated alterations of intratumoral NK cell phenotype and function in lung carcinoma. Cancer Res. 2011;71(16):5412–22.
18. Villegas FR, Coca S, Villarrubia VG, Jiménez R, Chillón MJ, Jareño J, et al. Prognostic significance of tumor infiltrating natural killer cells subset CD57 in patients with squamous cell lung cancer. Lung Cancer. 2002;35(1):23–8.
19. Halama N, Braun M, Kahlert C, Spille A, Quack C, Rahbari N, et al. Natural killer cells are scarce in colorectal carcinoma tissue despite high levels of chemokines and cytokines. Clin Cancer Res. 2011;17(4):678–89.
20. Ishigami S, Natsugoe S, Tokuda K, Nakajo A, Che X, Iwashige H, et al. Prognostic value of intratumoral natural killer cells in gastric carcinoma. Cancer. 2000;88(3):577–83.
21. Eckl J, Buchner A, Prinz PU, Riesenberg R, Siegert SI, Kammerer R, et al. Transcript signature predicts tissue NK cell content and defines renal cell carcinoma subgroups independent of TNM staging. J Mol Med (Berl). 2012;90(1):55–66.
22. Esendagli G, Bruderek K, Goldmann T, Busche A, Branscheid D, Vollmer E, et al. Malignant and non-malignant lung tissue areas are differentially populated by natural killer cells and regulatory T cells in non-small cell lung cancer. Lung Cancer. 2008;59(1):32–40.
23. Fauteux-Daniel S, Faure F, Marotel M, Geary C, Daussy C, Sun JC, et al. Styk1 expression is a hallmark of murine NK cells and other NK1.1(+) subsets but is dispensable for NK-cell development and effector functions. Eur J Immunol. 2019;49(5):677–85.
24. Ebrahimi N, Fardi E, Ghaderi H, Palizdar S, Khorram R, Vafadar R, et al. Receptor tyrosine kinase inhibitors in cancer. Cell Mol Life Sci. 2023;80(4):104.
25. Jiao Q, Bi L, Ren Y, Song S, Wang Q, Wang YS. Advances in studies of tyrosine kinase inhibitors and their acquired resistance. Mol Cancer. 2018;17(1):36.
26. Huang L, Jiang S, Shi Y. Tyrosine kinase inhibitors for solid tumors in the past 20 years (2001–2020). J Hematol Oncol. 2020;13(1):143.
27. Ilander M, Olsson-Strömberg U, Schlums H, Guilhot J, Brück O, Lähteenmäki H, et al. Increased proportion of mature NK cells is associated with successful imatinib discontinuation in chronic myeloid leukemia. Leukemia. 2017;31(5):1108–16.
28. Lowell CA. Src-family and syk kinases in activating and inhibitory pathways in innate immune cells: signaling cross talk. Cold Spring Harb Perspect Biol. 2011;3(3):a002352.
29. Damele L, Montaldo E, Moretta L, Vitale C, Mingari MC. Effect of tyrosin kinase inhibitors on NK cell and ILC3 development and function. Front Immunol. 2018;9:2433.

Publisher's note